Tracer Diffusion of Proteins in DNA Solutions. 2. Green Fluorescent Protein in Crowded DNA Solutions

Nathan A. Busch, Thomas Kim, and Victor A. Bloomfield*

Department of Biochemistry, Molecular Biology, and Biophysics University of Minnesota, 1479 Gortner Avenue, Saint Paul, Minnesota 55108

Received March 30, 2000; Revised Manuscript Received June 7, 2000

ABSTRACT: Proteins diffuse to their sites of action within cells in a crowded, strongly interacting environment of nucleic acids and other macromolecules. To investigate the dynamics of a typical globular protein in such an environment, we used fluorescence photobleaching recovery to measure the probe diffusion of green fluorescent protein (GFP) in dilute to highly concentrated aqueous solutions of glycerol, Ficoll 70, and persistence-length calf thymus DNA. In glycerol, GFP accurately obeyed the Stokes−Einstein equation that relates diffusion coefficient to solution viscosity. In concentrated Ficoll 70, GFP diffused moderately faster than predicted from viscosity, demonstrating the phenomenon of microviscosity in a molecularly heterogeneous solution. In DNA, the diffusion coefficient of GFP was markedly greater than predicted from the Stokes−Einstein equation, with deviations increasing at lower ionic strength. This behavior reflects microviscosity, Coulombic interactions, and the dynamics of probe diffusion in DNA solutions that had undergone the ordinary−extraordinary transition, which we demonstrated by dynamic light scattering.

Introduction

Intracellular regulatory proteins find their DNA binding sites in a crowded, strongly interacting environment of DNA and other macromolecules. We wish to understand how proteins diffuse in such an environment, and how weak, nonspecific interactions affect diffusion to a specific binding target. In paper 1 in this series,[1] we used fluorescence photobleaching recovery (FPR) to measure the probe diffusion coefficient of fluorescein−5-isothiocyanate-labeled bovine serum albumin (FITC−BSA) in DNA solutions of relatively low to moderate concentration (up to 38 mg/mL or 2% volume fraction). By comparing solutions of 0.01 and 0.1 M ionic strength, we concluded that electrostatic interactions between the probe and DNA play a significant role in probe diffusion.

In this paper we explored more deeply the factors influencing probe diffusion, by making observations over a broader range of conditions. We used a higher range of DNA concentrations, from 7 to 85 mg/mL, and varied NaCl concentration from nominally salt-free to 200 mM. In systems of high DNA concentrations and/or low ionic strength, long-range ordering is known to occur.[2−9] To distinguish effects of long-range ordering from those of high viscosity and crowding, we measured probe diffusion diffusion coefficients in solutions of DNA, Ficoll, and glycerol. We used dynamic laser light scattering to measure the diffusional behavior of the DNA solution itself. To eliminate the possibility that part of the fluorescence recovery signal comes from FITC unbound to protein, we used green fluorescent protein (GFP), which is smaller than BSA (M_r = 27 kDa compared to 66 kDa) but has similar charge at pH 7 (−20 compared to −16).

We found that in glycerol GFP accurately obeyed the Stokes−Einstein equation that relates diffusion coefficient to solution viscosity. In concentrated Ficoll 70, GFP diffused about 50% faster than predicted from the viscosity of the solution. This is attributable to the phenomenon of microviscosity in a molecularly heterogeneous solution. In DNA, the diffusion coefficient of GFP was as much as 5-fold greater than predicted by the Stokes−Einstein equation, with greater deviations and a different functional form at lower ionic strength. We showed by dynamic light scattering that the DNA solutions had undergone to greater or lesser extent the ordinary−extraordinary transition.[2,7−9] The probe diffusion behavior therefore presumably reflects microviscosity, Coulombic repulsions between the GFP and DNA, and the dynamics of probe diffusion in DNA solutions that themselves showed both fast and slow diffusion processes.

Materials and Methods

Buffers. Phosphate-buffered saline (PBS): 0.15 M NaCl, 0.01 M KH_2PO_4, 0.01 M K_2HPO_4, pH 7.0. Tris: Tris[hydroxymethyl]aminomethane. EGTA: Ethylene glycol-bis-β-aminoethyl ether. TE: Tris/EGTA, 10 mM Tris, 1 mM EGTA, pH 7.0.

Ficoll 70 was purchased from Pharmacia Biotechnology and used without further purification. Properties of Ficoll solutions have been described previously.[10] Glycerol was obtained from Fisher Scientific.

Green Fluorescent Protein, GFP. Recombinant green fluorescent protein (EGFP, Phe64Leu, Ser65Tyr) from ClonTech, Palo Alto, CA, was extensively dialyzed against TE buffer, concentrated to ∼1 mg/mL, stored at 4 °C, and used without further purification. Probe concentration was well below 0.1 mg/mL to avoid GFP−GFP interactions.

Calf Thymus DNA. Approximately 12 g of calf thymus DNA (CT-DNA), nominally 160 base pairs in length, was produced according to a previously published protocol.[11] The CT-DNA produced by the standard protocol yields a fairly broad distribution of sizes (120− 200 base pairs).[12] To narrow the size distribution, the DNA was fractionated on a Sephacryl S-400 (2.5 × 96 cm Pharmacia) chromatography column with a 170 base pair cutoff for DNA. The column was equilibrated with PBS, and the running buffer was PBS. Each fraction was then analyzed by SDS-PAGE, and those fractions with sizes 160 ± 10 base pairs were pooled, extensively dialyzed, and concentrated using stirred ultrafiltration. The concentrated

* Corresponding author. E-mail: victor@tc.umn.edu.

10.1021/ma0005724 CCC: $19.00
Published on Web 07/18/2000

CT-DNA was then purified on a Sephacryl S-300 (2.5 × 96 cm Pharmacia) chromatography column which was equilibrated using TE buffer; the running buffer was also TE. The peak corresponding to 160 base pairs was concentrated to 100 mg/mL and stored at 4 °C. The resulting CT-DNA solution was characterized by several techniques. First, both protein and phenol contamination were determined to be negligible since $A_{260}/A_{280} = 1.90$ and $A_{260}/A_{270} = 1.22$, both ratios well within accepted ranges for DNA purity.[13] Second, the size distribution for the CT-DNA was determined using SDS-PAGE, with a 123 base pair ladder (Gibco BRL) standard. Third, dynamic light scattering at low DNA concentration was used to characterize the mean hydrodynamic radius and polydispersity. Also, CONTIN analysis (see below) of the dynamic light scattering data yielded a size distribution which correlated well with that determined using SDS-PAGE.

Fluorescence Photobleaching Recovery. Fluorescence photobleaching recovery measurements were performed to measure the tracer diffusion coefficient in a variety of backgrounds including both extremely viscous and crowded solutions. An argon ion laser operated at 488 nm (model 95-3, Lexel Corp., Fremont, CA) was used for photobleaching and probing.

The laser beam was attenuated with an acousto-optic modulator (model N35085-3, Neos Technologies, Melbourne, FL) and a set of neutral density filters such that the probe beam intensity was $\sim 1 \times 10^{-4.4}$ relative to the photobleaching beam intensity. A pellicle beam splitter (Oriel Corporation, Stratford, CA) was used to deflect a small fraction of the laser beam to a detector (model 822, Newport Instruments) for monitoring the laser stability. The balance of the laser light was directed to a Nikon Labphot-2 microscope via a single beam steering mirror. The auxiliary light source adapter for the microscope was fitted with an iris which allowed the formation of a well-defined spot, with a sharp border between the illuminated region and the black non-illuminated region on the fluorescent sample. A dichroic mirror was used to direct the laser light to the sample while permitting the fluorescent light to pass through to the photomultiplier tube. The laser, optics, and microscope were mounted on an optical instrument table for stability and vibration isolation.

The sample consisted of a 100 μm thick layer of solution sandwiched between two microscope slides separated by a 0.1 mm stainless steel spacer. This arrangement permitted control over the thickness of the sample film as well as constraining the film against movement during both photobleaching and fluorescence recovery.

Since the temperature of the FPR environment fluctuated between experimental trials, we monitored the temperature with a thermocouple accurate to ±0.05 °C.

To perform the FPR experiment, the sample slide was placed onto the stage of a fluorescence microscope which contained a 488/519 nm dichroic mirror, a photomultiplier tube (S982, Hamamatsu, Inc., Bridgewater, NJ) for measuring the fluorescent photons, and an iris to window the excitation laser beam. The current from the PMT was converted to a voltage via a 94 kΩ resistive short across the positive and ground terminals of the PMT and amplified (model SR560 Preamplifier, Stanford Research Systems, CA) before being measured and stored to a computer disk. The voltage was monitored by an A/D converter circuit (NB-MIO-16, National Instruments, TX) using LabView (National Instruments) on a Macintosh IIfx computer. The windowing of the excitation beam by the iris permitted control over the area of illuminated sample as well as accurate measurement of the diameter of this illuminated area.

At the high viscosities and polymer concentrations used in our experiments, the probe diffusion coefficient was significantly reduced. Therefore, FPR experiments often took in excess of 30− 45 min to complete. To minimize photobleaching damage to the fluorophore, the FPR instrument was modified so that the probe beam could be shuttered to allow illumination intervals as short as 50− 60 ms. During the longer fluorescence recovery phases, the sample was illuminated for $^1/_2$ s every 10 s.

Probe diffusion coefficients D were determined from

$$\tau = \frac{a^2}{4D} \tag{1}$$

where a, the radius of both the bleaching and probe spot, was determined by optical micrometry to be 50 μm, and the characteristic fluorescence recovery time τ is defined by the residual fluorescence fraction[14]

$$r(t) = \frac{F(t) - F(\text{dark})}{F(-) - F(\text{dark})} = \exp\left[-\frac{2}{1 + 2\tau/t}\right] \tag{2}$$

where $F(-)$ and $F(\text{dark})$ are the fluorescence intensities immediately before and after bleaching.

We verified by direct measurement with a thermocouple placed adjacent to the bleached spot that there was no significant temperature rise from the adsorption of the bleaching beam and therefore no effect on the viscosity of the solution or diffusion coefficient of the probe. All FPR experiments were done as close as possible to 20 °C.

Dynamic Light Scattering. The dynamic light scattering measurements were carried out on a turntable and goniometer (model RR54, Precision Devices, Ltd., Malvern, U.K.) using the 488 nm line of an argon ion laser for DNA and the 632.5 nm line from a helium−neon laser for GFP. The photon autocorrelation function[15] was measured by a BI-9000-AT correlator (Brookhaven Instrument Corporation, Holtsville, NY) and recorded for analysis by an IBM PC/AT microcomputer. The laser and goniometer were mounted on an optical instrument table. The index matching fluid and sample cell were maintained at constant temperature ±0.1 °C by continuously circulating water from a water bath (model D1/G, Haake, Berlin, Germany).

Solutions were cleaned of dust in situ using a recirculating 0.2 μm Millipore filter system. The sample cell contained ~2 mL of solution which was filtered at approximately 1 mL/min for 20 min. During the measurement, residual dust in the solution was detected by continuously monitoring the total intensity of scattered light and rejecting any sequence in which the intensity fluctuated from the mean value by more than 3%.

To encompass a wide dynamic range, we recorded the intensity autocorrelation function for a duration of 200 s at various correlator sample times which depended upon the scattering angle. Typically, the scattering angles and sample times were 90° (1, 2, 5, 10, and 20 μs), 60° (1, 2, 5, 10, 20, and 50 μs), and 45° (5, 10, 20, 50, 100, and 200 μs). However, other scattering angles were also employed as necessary. At the end of each measurement, the total average intensity and autocorrelation function were recorded on disk for further analysis.

Autocorrelation functions were analyzed in three ways. The method of cumulants[16] was used to determine the z-average diffusion coefficient D_z and polydispersity index. CONTIN analysis[17] yielded the distribution of diffusion coefficients. A method of analysis assuming a finite number of exponential decay processes was used to dissect scattering from concentrated DNA solutions into slow and fast diffusional modes. Hydrodynamic radii R_h were obtained from diffusion coefficients D by the Stokes−Einstein equation

$$D = \frac{kT}{6\pi\eta R_h} \tag{3}$$

where k is the Boltzmann constant, T the temperature, and η the solvent viscosity.

Densimetry and Viscometry. Densities and viscosities were measured as described previously.[18] Densities of solutions were measured with a Mettler/Paar precision density meter DMA 020 (accurate to 10^{-6} g/mL) and Hotpack water bath (accurate to ±0.01 °C).

Viscosities were determined with Cannon-Ubbelohde semimicro type 75 and 100 viscometers in a Hotpack water bath. Stop watches (readable to ±0.1 s) used for timing compared

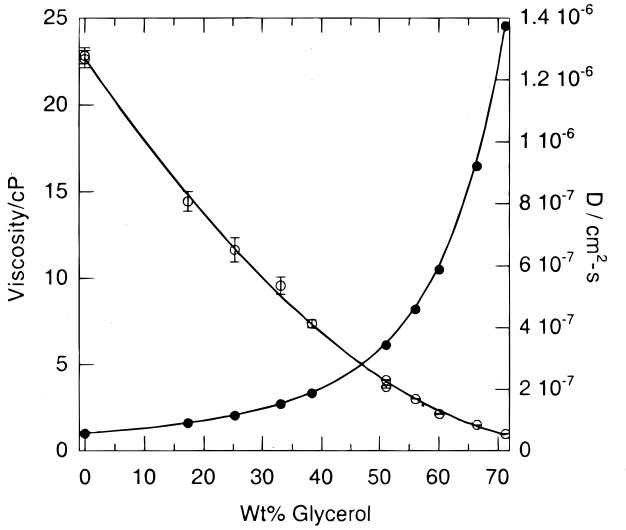

Figure 1. Viscosity of glycerol solutions (●) and diffusion coefficient of GFP in glycerol as measured by FPR (○) as functions of the weight percent of glycerol in the solution.

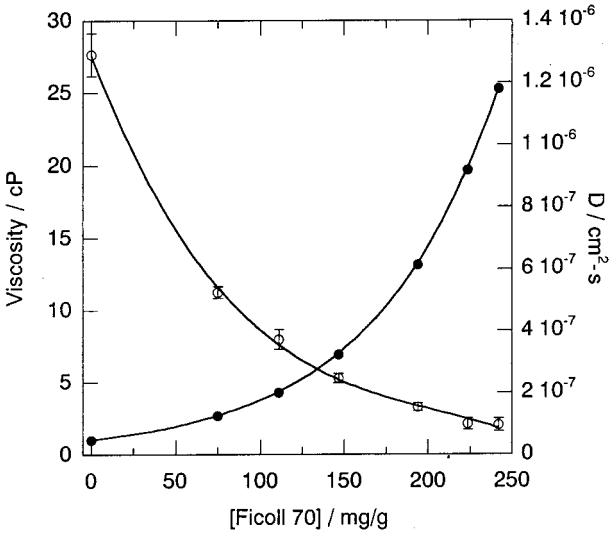

Figure 2. Viscosity of Ficoll 70 solutions (●) and diffusion coefficient of GFP in Ficoll 70 as measured by FPR (○) as functions of the concentration of Ficoll (mg/g).

exactly over 30 min intervals with traceable digital timers (±1 s) calibrated to ±0.01%. Glycerol densities and viscosities were in good agreement with handbook values.[19]

Results

Hydrodynamic Radius of GFP. We employed two techniques to determine the hydrodynamic radius of GFP. First, dynamic light scattering at 632.5 nm was used to obtain 15.8 ± 0.2 Å as the hydrodynamic radius in TE, pH 7.0. Second, FPR measurements were performed on GFP in glycerol−water solutions with glycerol concentrations of 0, 17.31, 25.32, 33.10, 38.38, 51.07, 56.13, 60.05, 66.38, and 71.26 wt %. The recovery time was measured, with 10 replications at each concentration, and converted to a diffusion coefficient according to eq. 1. In all cases, the FRAP recovery traces were accurately represented by a single recovery time indicating only a single identifiable diffusing species.[14,20] The Stokes−Einstein equation then gave a hydrodynamic radius of 16.6 ± 0.8 Å, independent of glycerol concentration.

Diffusion of GFP in Glycerol, Ficoll 70, and DNA Solutions. The overall goal of this research is to determine whether proteins interact with crowded DNA solutions in a distinctive way. GFP is not a DNA-binding protein or enzyme, so we do not expect any specific chemical interaction. However, it is negatively charged, as is DNA, so we would expect to see some evidence of electrostatic interaction. We therefore carried out FPR experiments with GFP in three solutions: glycerol, which contributes high viscosity; Ficoll 70, which contributes both high viscosity and crowding; and DNA, which contributes viscosity, crowding, and electrostatics. The results are shown in Figures 1− 3, which display both the viscosity and GFP diffusion coefficient as a function of concentration in each of the three types of solution.

In Figure 4 we plot the ratios of the observed diffusion coefficients to those expected if the Stokes−Einstein equation were obeyed. As expected, GFP in glycerol solutions shows classic Stokes−Einstein behavior. The same is not true, however, for the other solutions. GFP in Ficoll 70 shows moderate deviations from Stokes−Einstein behavior, particularly at higher Ficoll concentrations and viscosities. This behavior is not uncommon

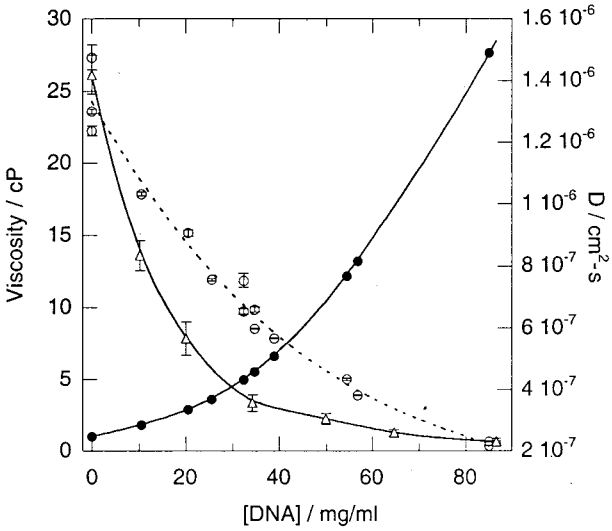

Figure 3. Viscosity of calf thymus DNA solutions (●) and diffusion coefficient of GFP in DNA without added salt (○) and in 150 mM NaCl (△) as measured by FPR as functions of the concentration of DNA (mg/mL).

in crowded solutions and indicates that the probe is sampling the microviscosity of the local environment rather than the macroviscosity of the solution as a whole.

Deviations from Stokes−Einstein (SE) behavior are much more dramatic in DNA solutions, as shown in Figure 4 as a function of viscosity and in Figure 5 as a function of DNA concentration. The dependence of GFP diffusion coefficient on [DNA] is approximately linear in solutions with no added salt:

$$D/D_{SE} = 1.081 + 0.0456[\mathrm{DNA}] \qquad (4)$$

while for DNA solutions with 150 mM NaCl, the dependence of D/D_{SE} on DNA concentration is approximately quadratic.

The results can also be written in stretched exponential form,

$$D/D_0 = \exp(-\alpha[\mathrm{DNA}]^{\nu}) \qquad (5)$$

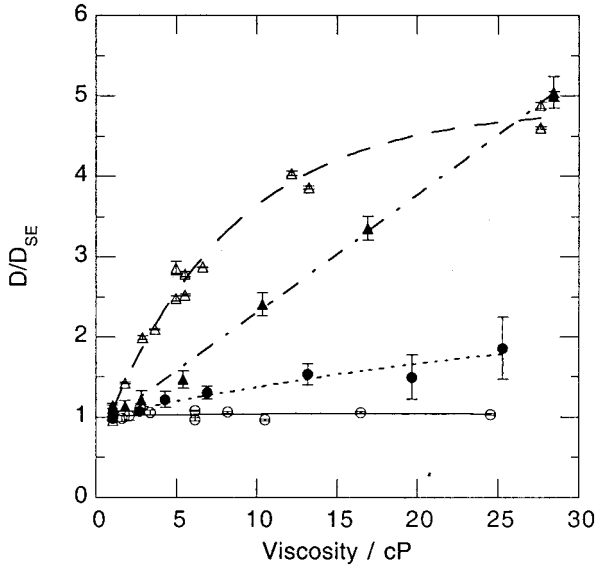

Figure 4. Ratio of the diffusion coefficients D obtained from FRAP measurements to those predicted by the Stokes–Einstein relation D_{SE} for GFP/glycerol/TE (○), GFP/Ficoll 70/TE (●), GFP/CT- DNA/TE + 150 mM NaCl (▲), and GFP/CT-DNA/TE with no added salt (△), as functions of the solution viscosity.

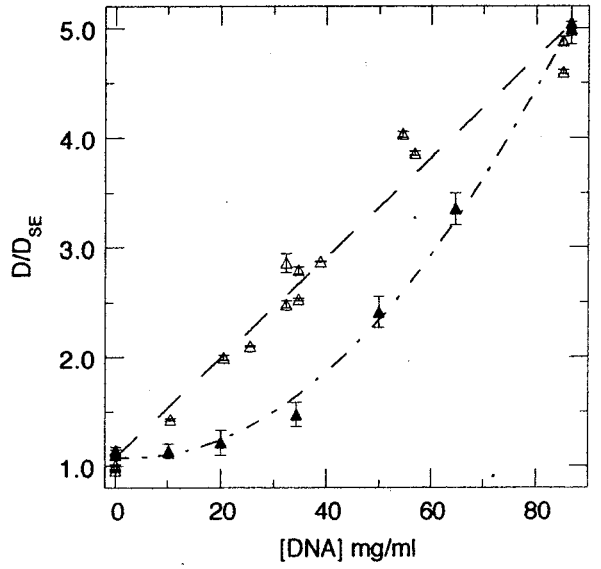

Figure 5. Ratio of the diffusion coefficients D obtained from FRAP measurements to those predicted by the Stokes–Einstein relation D_{SE} for GFP in CT- DNA/TE + 150 mM NaCl (▲) and in CT-DNA/TE with no added salt (△), as functions of the DNA concentration.

where D_0 is the probe diffusion coefficient in buffer alone. In DNA solutions with no added salt, we found $\nu = 0.997$ and $\alpha = 0.022$. These parameters are in excellent agreement with those obtained previously with BSA as probe:[1] $\nu \approx 1$ and $\alpha = 0.018 \pm 0.006$ and 0.024 ± 0.007 in 0.1 and 0.001 M NaCl buffers, respectively. The ionic strength of TE buffer at pH 7.0 is approximately 10 mM, and the contribution of the uncondensed counterions to the ionic strength of the DNA solution with no added salt is 3.6 mM in 10 mg/mL DNA and 31 mM in 85 mg/mL. In contrast, however, our data for GFP diffusion in DNA with 150 mM NaCl buffer are best fit to a stretched exponential with $\nu = 0.56$ and $\alpha = 0.16$.

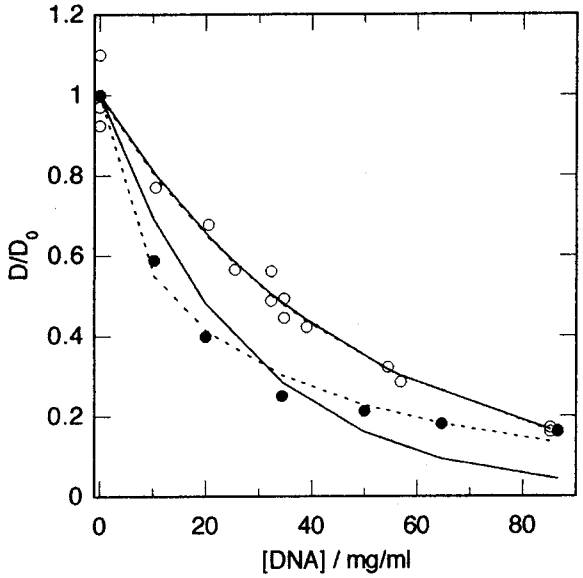

Figure 6. Ratio of the diffusion coefficients D obtained from FRAP measurements at finite DNA concentrations to those D_0 at zero concentration (buffer only) for GFP in CT- DNA/TE with no added salt (○) and in CT- DNA/TE + 150 mM NaCl (●). The lines are best fits to accessible volume (—) and stretched exponential (···) equations. In the solutions with no added salt, the two equations essentially coincide.

Fits with these parameters are shown in Figure 6. Neither the fit nor the agreement with our earlier BSA results in 0.1 M NaCl is very good. The diffusion coefficient of GFP decreases considerably more rapidly with DNA concentration than did the diffusion coefficient of BSA, although the salt concentrations were similar. In fact, the diffusion coefficient for GFP in 150 mM NaCl–DNA solutions is lower than for GFP in DNA solutions with no added salt, in contrast to our previous results with BSA.[1]

Another useful representation of the data is the accessible volume model.[1,21] The ratio of the diffusion coefficient in a solution occupied by background fibers to that in buffer alone is assumed proportional to the unoccupied volume fraction:

$$D/D_0 = 1 - \phi \tag{6}$$

where ϕ is the fractional volume occupied. The probability of being able to accommodate a spherical particle of radius R in a background of randomly oriented rigid fibers of length F and negligible thickness is[21]

$$1 - \phi = \exp\left[-\left(\pi n F R^2 + \frac{4}{3}\pi n R^3\right)\right] \tag{7}$$

where n is the number density of fibers. A DNA length of 544 Å (160 bp × 3.4 Å per bp) was used for F. The best-fit values of R were 47 Å in no added salt and 61 Å in 150 mM salt, but the fit to the accessible volume model in the latter case was quite poor, as seen in Figure 6.

To gain some insight into the structure of the DNA solutions that may be causing the strongly anomalous diffusion seen in those solutions, we conducted dynamic light scattering on pure 160 bp CT-DNA/TE systems as a function of NaCl (0, 50, 100, 150, and 200 mM) and DNA (1, 5, and 10 mg/mL) concentrations. The diffusion coefficients obtained at 90° scattering angle, shown in Figure 7, clearly indicate the presence of two diffusional

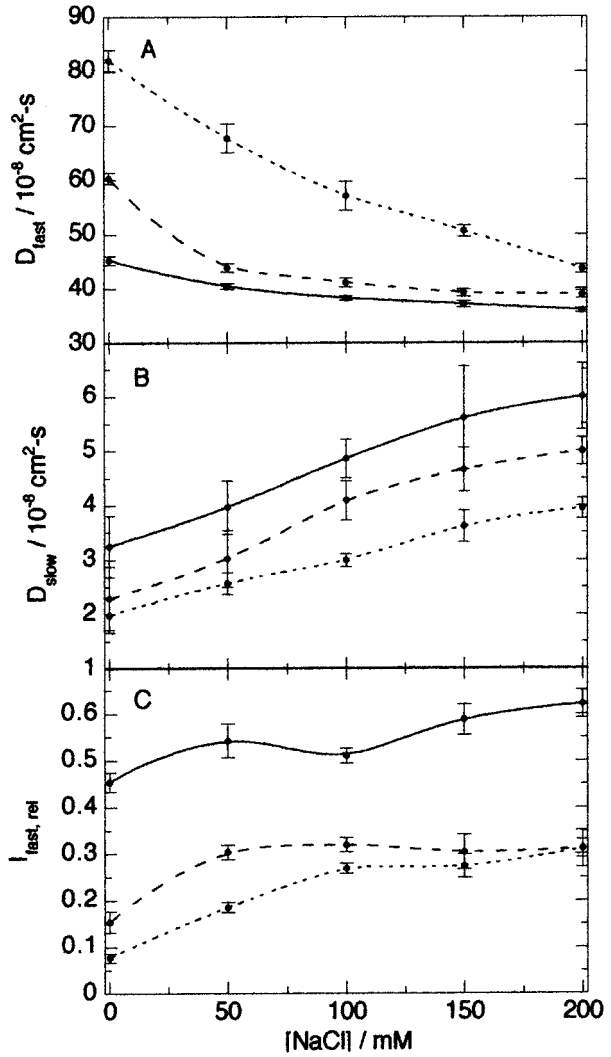

Figure 7. Fast (A) and slow (B) mode diffusion coefficients of 160 bp calf thymus DNA as functions of added NaCl concentration and DNA concentrations of 1 mg/mL (—), 5 mg/mL (– –), and 10 mg/mL (···). The normalized fast component intensity is given in panel C.

modes, as we and others have observed previously.[2,7–9] This has been termed the "ordinary–extraordinary" transition, first observed in polylysine.[22,23] The slow diffusion mode is the signature of the extraordinary phase.

The apparent fast component diffusion coefficient D_{fast}, shown in panel A of Figure 7, increases with increasing DNA concentration, while the slow component diffusion coefficient, D_{slow}, decreases (panel B) with increasing CT-DNA concentration. The normalized intensity for the fast mode, I_{fast}, falls off at low ionic strength for all DNA concentrations investigated (panel C). These results suggest the presence of large-scale structures in the solution, especially prominent at low ionic strength, along with the monomeric CT-DNA.

Our FPR experiments show that the depth of the residual fluorescence as defined by $r(t)$ in eq 2 is independent of the CT-DNA concentration. Over the range of glycerol concentrations from 0 to 71 wt %, $r(0)$ (the fraction of initially unbleached GFP) is 0.23 ± 0.02, independent of glycerol concentration, while for DNA concentrations from 0 to 85 mg/mL, $r(0) = 0.21 \pm 0.02$, also independent of concentration. Likewise, at t equal to 10 times the fluorescence recovery time, $r(10\tau) = 0.90 \pm 0.04$ for both glycerol and DNA solutions, independent of concentrations over the same ranges. If the GFP were being partitioned into separate microscopic phases within the DNA or were becoming entrapped in a DNA gel at higher concentrations, then we would expect that $r(10\tau)$ and possibly $r(0)$ would vary systematically with CT-DNA concentration. Since this is not the case, we conclude that most of the GFP is not being trapped in the CT-DNA background. This is consistent with the fact that the DNA did not physically gel (i.e., it remained pourable), as it does at low temperatures.[3]

In summary, we see that concentrated Ficoll solutions produce modest deviations from ideal Stokes–Einstein behavior, presumably due to excluded-volume and/or microviscosity effects. DNA produces much larger deviations, of which some proportion is probably also due to excluded volume and microviscosity. However, the additional strong increase in diffusion coefficient of GFP with increasing CT-DNA concentration must be attributed to electrostatic interactions between protein and DNA or to poorly understood aspects of the extraordinary phase of DNA.

Discussion

We have studied the diffusion of GFP, a small probe protein, in aqueous solutions of three quite different types of molecules: glycerol, Ficoll 70, and 160 bp calf thymus DNA. Glycerol is a small cosolvent that strongly raises the solution viscosity but does not fundamentally change solution dynamics: the diffusion coefficient of GFP in glycerol obeys Stokes–Einstein behavior. Ficoll is a cross-linked copolymer of sucrose and epichlorohydrin; it is electrically neutral and has a compact, rigid structure due to cross-linking.[25] The sample of Ficoll 70 that we used has a number-average molecular weight of about 75 kDa and an average Stokes radius of 5.5 nm.[10] GFP diffuses faster in Ficoll 70 solutions than would be predicted from the macroscopic viscosity of these solutions, but the deviations from Stokes–Einstein behavior are relatively moderate, less than a factor of 2 at the highest Ficoll concentrations. Such behavior is not uncommon and is plausibly attributed to microviscosity in a molecularly heterogeneous solution.

Deviations from Stokes–Einstein behavior are much greater in DNA solutions. In part this may be due to the rodlike character of the DNA (160 bp DNA is about one persistence length long, so it is a gently bending rod). Rods will raise the viscosity of a solution more than spherical molecules at the same concentration, as is evident from comparison of Figures 2 and 3. Therefore, it might be expected that the regions in a solution of rods in which the local environment is essentially that of low-viscosity buffer are larger than in a solution of spheres, allowing more rapid diffusion in DNA than in Ficoll. This may explain much of the difference between DNA and Ficoll in Figure 4, but it is clear that the ionic strength of the DNA solution also plays a role, indicating an important electrostatic contribution.

In our previous results on the diffusion of FITC-labeled BSA in DNA,[1] the maximum DNA concentration was 35 mg/mL. In this study with GFP, we went to 85 mg/mL DNA, emphasizing conditions that spotlight nonideal behavior. Comparison of the two systems reveals two striking differences. First, the diffusion coefficient of GFP is greater in low salt than in high salt DNA solutions, while for FITC-BSA the opposite is

true. Second, the exponent ν in the stretched exponential fit to eq 5, while ≈ 1 in low salt DNA solutions for both proteins, is 0.56 for GFP in 0.15 M NaCl but also ≈ 1 for BSA in 0.1 M NaCl. We have no ready explanation for these differences, though they may arise in part from the greater size of BSA relative to GFP. (There may also have been some free FITC in the BSA solutions, since the attachment to the protein is noncovalent. However, it is not clear whether this would vary with ionic strength.) We observe, however, that a value of $\nu \sim 0.5$ was found for diffusion of a spherical probe in solutions of a rodlike polymer,[26] consistent with our present high salt results.

In the earlier paper we rationalized the lower diffusion coefficient in low salt as resulting from the more extended Debye−Hückel ion atmosphere around the DNA, causing an increase in effective excluded volume due to the "thickening" of the DNA double helix. Clearly, that explanation does not apply to our present results with GFP. The effective radius R of the protein, which is actually the sum of the effective radii of sphere and background rodlike fibers (since in the accessible volume model the fibers have zero radius), is smaller in low salt than in high salt.

It is also worth considering that if there is electrostatic repulsion between DNA and protein (both are negatively charged at neutral pH), protein diffusion should be speeded up by the repulsive force even as it is retarded by a greater effective excluded volume. The balance of these two effects may be different for GFP and BSA.

The results in Figure 7 show that the extraordinary phase, associated with a slow diffusion process, exists in DNA solutions with no added salt even at the lowest DNA concentrations we studied. This was presumably also the case in our earlier work,[1] though it was not recognized there. The nature of the extraordinary phase—which occurs in a variety of synthetic polyelectrolytes as well as in DNA (see, e.g., Chapter 7 of the book by Schmitz[27])—has been the subject of much debate. It is important to note that the ordinary−extraordinary transition appears mainly in the mutual diffusion coefficient measured by dynamic light scattering. In particular, it is not manifested in a large increase in the solution viscosity,[28] as is clear from Figure 3.

Normally, it is assumed that slow translational diffusion means large particles in solution. Despite the puzzling fact that appearance of the extraordinary phase in DNA solutions is not accompanied by the increase in scattering intensity that would be expected if large particles are formed,[2] and despite debates about whether such large structures are filterable impurities,[29,30] evidence for equilibrium large-scale structures has been obtained.[31] Probably most workers in the field believe that the extraordinary phase represents the slow diffusion of large molecular aggregates stabilized largely by weak collective electrostatic interactions. We provisionally accept this interpretation, even though the ordinary−extraordinary transition in DNA does not obey the rules of small ion concentration and valence that have been formulated for flexible polyelectrolytes.[9]

Two possibilities suggest themselves to describe the nature of the 160 bp CT-DNA background. Either the CT-DNA behaves as a homogeneous sol−gel and the protein can only diffuse through the gel matrix by displacing CT-DNA molecules, or the CT-DNA forms a heterogeneous sol−gel and the protein is free to diffuse along essentially CT-DNA-free channels through larger regions of more concentrated DNA. The homogeneous sol−gel picture seems inconsistent with the maintenance of a finite viscosity, and the heterogeneous sol−gel model seems more consistent with the prevalent picture of the extraordinary phase. In either case, it is likely that a significant contribution to the unusually large non-Stokes−Einstein diffusional behavior of the probe in these solutions comes from the dynamics of the background DNA phase.

Acknowledgment. This research was supported in part by grants from the National Science Foundation.

References and Notes

(1) Wattenbarger, M. R.; Bloomfield, V. A.; Bu, Z.; Russo, P. S. *Macromolecules* **1992**, *25*, 5263− 5265.
(2) Fulmer, A. W.; Benbasat, J. A.; Bloomfield, V. A. *Biopolymers* **1981**, *20*, 1147− 1159.
(3) Fried, M. G.; Bloomfield, V. A. *Biopolymers* **1984**, *23*, 2141− 2155.
(4) Rill, R. L.; Hilliard, P. R., Jr.; Levy, G. C. *J. Biol. Chem.* **1983**, *258*, 250− 256.
(5) Strzelecka, T. E.; Rill, R. L. *J. Am. Chem. Soc.* **1987**, *109*, 4513− 4518.
(6) Strzelecka, T. E.; Rill, R. L. *Biopolymers* **1990**, *30*, 57− 71.
(7) Schmitz, K. S.; Lu, M. *Biopolymers* **1984**, *23*, 797−808.
(8) Nicolai, T.; Mandel, M. *Macromolecules* **1989**, *22*, 2348− 2356.
(9) Ferrari, M. E.; Bloomfield, V. A. *Macromolecules* **1992**, *25*, 5266− 5276.
(10) Wenner, J. R.; Bloomfield, V. A. *Biophys J.* **1999**, *77*, 3234− 3241.
(11) Wang, L.; Ferrari, M.; Bloomfield, V. A. *BioTechniques* **1990**, *9*, 24− 27.
(12) Kassapidou, K.; Jesse, W.; Vandijk, J.; van der Maarel, J. R. C. *Biopolymers* **1998**, *46*, 31− 37.
(13) Liebe, D. C.; Stuehr, J. E. *Biopolymers* **1972**, *11*, 167− 184.
(14) Jacobson, K.; Wu, E.; Poste, G. *Biochim. Biophys. Acta* **1976**, *433*, 215− 222.
(15) Berne, B. J.; Pecora, R. *Dynamic Light Scattering with Applications to Chemistry, Biology, and Physics*; Wiley-Interscience: New York, 1976; 376 pp.
(16) Koppel, D. E. *J. Chem. Phys.* **1972**, *57*, 4814− 4820.
(17) Provencher, S. W. *Comput. Phys. Commun.* **1982**, *27*, 229− 242.
(18) Wenner, J. R.; Bloomfield, V. A. *J. Biomol. Struct. Dyn.* **1999**, *17*, 461− 471.
(19) Weast, R. C.; Astle, M. J. *CRC Handbook of Chemistry and Physics*; CRC Press: Boca Raton, FL, 1985.
(20) Axelrod, D.; Koppel, D. E.; Schlessinger, J.; Elson, E.; Webb, W. W. *Biophys. J.* **1976**, *16*, 1055− 1069.
(21) Ogston, A. G.; Preston, B. N.; Wells, J. D. *Proc. R. Soc. London A* **1973**, *333*, 297− 316.
(22) Lee, W. I.; Schurr, J. M. *J. Polym. Sci., Polym. Phys. Ed.* **1975**, *13*, 873− 888.
(23) Lin, S.-C.; Lee, W. I.; Schurr, J. M. *Biopolymers* **1978**, *17*, 1041− 1064.
(24) Stigter, D. *Biopolymers* **1979**, *18*, 3125− 3127.
(25) Bohrer, M. P.; Patterson, G. D.; Carroll, P. J. *Macromolecules* **1984**, *17*, 1170− 1173.
(26) Tracy, M. A.; Pecora, R. *Macromolecules* **1992**, *25*, 337− 349.
(27) Schmitz, K. S. *Macroions in Solution and Colloidal Suspension*; VCH Publishers: New York, 1993.
(28) Martin, N. B.; Tripp, J. B.; Shibata, J. H.; Schurr, J. M. *Biopolymers* **1979**, *18*, 2127−2133.
(29) Ghosh, S.; Peitzsch, R. M.; Reed, W. F. *Biopolymers* **1992**, *32*, 1105− 1122.
(30) Sedlak, M. *Macromolecules* **1995**, *28*, 793− 794.
(31) Ermi, B. D.; Amis, E. J. *Macromolecules* **1998**, *31*, 7378− 7384.

MA0005724